XVI International Conference on Computational Plasticity. Fundamentals and Applications
COMPLAS 2021
E. Oñate, D. Peric, M. Chiumenti and Eduardo de Souza Neto (Eds)

3D FINITE ELEMENT MODEL FOR PREDICTION OF THE HOT ROLLED STRIP CROWN AND ROLL DEFORMATION

ARIF HAMDAM*, MITSUHIKO SANO†, MASASHI TSUGENO† AND KAZUHIRO OHARA†

*† Toshiba Mitsubishi-Electric Industrial Systems Corporation (TMEIC)
3-1-1 Kyobashi, Chuo-ku, Tokyo 104-0031, Japan
E-mail: HAMDAM.Arif@tmeic.co.jp, Web page: http://www.tmeic.com

Key words: FEM, Rolling Process, Hot Strip Mill, Strip Crown, Roll Profile.

1 INTRODUCTION

In a hot strip mill (HSM), the strip crown is one of the most important parameters which evaluate the quality of hot rolled strip. If the strip crown is not appropriate, the downstream process becomes unstable, and defects may occur in the products. Therefore, it is desired to improve the accuracy of strip crown control.

In a HSM, various factors such as the roll crown, deflection and flattening of the roll due to the rolling force, thermal expansion of rolls due to contact between the roll and strip and changes in roll wear have a strong effect in the strip crown. On the other hand, rolling mills have crown control actuators such as work roll benders. To control the strip crown precisely using these actuators, an improved accuracy of strip crown prediction is required.

In the past several decades, different numerical calculations have been applied to study the deformation of the roll set, including the elastic base beam method introduced by Stone [1] and the influence function method proposed by Shohet and Townsend [2]. In Shohet's method (split model), the axial directions of the work roll (hereinafter WR), backup roll (hereinafter BUR) and strip are divided into a large number of small elements. In this method, it is possible to solve the equilibrium condition with the rolling force acting on the contact part and calculate the deflection of WR and BUR with relatively high accuracy. However, a simple theory is used for contact stress distribution in the width direction and the accuracy of WR flattening deformation is not sufficient.

Yanagimoto et al. [3] developed a combined one-dimensional split model and FEM (CORMILL system) by using computer resources to calculate the strip crown with good accuracy. In the CORMILL system, a one-dimensional split model is used to calculate the deflection of the WR and BUR, and a 3D rigid-plastic FEM is used to calculate the deformation and rolling force of the strip. Furthermore, in recent years, several studies were conducted to calculate the strip crown by using rigid-plastic FEM [4, 5]. In rigid-plastic FEM, it is assumed that the elastic strain in strip side is small, and that elastic deformation will not occur. This assumption may cause a prediction error due to elastic deformation of the strip that occurs before and after the roll contact part.

In this study, we have developed a 3D FEM model for a 4-High finishing rolling mill using three-dimensional elasto-plastic finite element method (FEM) for strip and elastic deformation for WR and BUR. The simulation was performed with flat strip, strip with entry crown and WR with initial crown. The strip crown was calculated for each case. By using the FEM simulation results, we have calculated the crown ratio heredity coefficient and transcription coefficient as used in the online strip crown model to control the strip crown in hot rolling process. Moreover, the effect of bending force in WR and backward tension on strip crown has been evaluated.

2 HOT STRIP ROLLING PROCESS

Figure 1 shows an example of conventional hot rolling mill [6]. The conventional mill consists of reheating furnace, edger, roughing mill, finishing mill, run-out cooling system and down coiler. In this study we have only focused on the finishing mill. HSM includes 6 or 7 finishing stands, which reduce the thickness of the transfer bar to the target thickness. The interstand tension can be controlled by adjusting the roll speed or the torque of loopers. A device called a WR bender, which consists of hydraulic cylinders to apply bending force between necks of top and bottom WRs, is installed to control the WR elastic axial deflection and the crown of the strip (Figure 2).

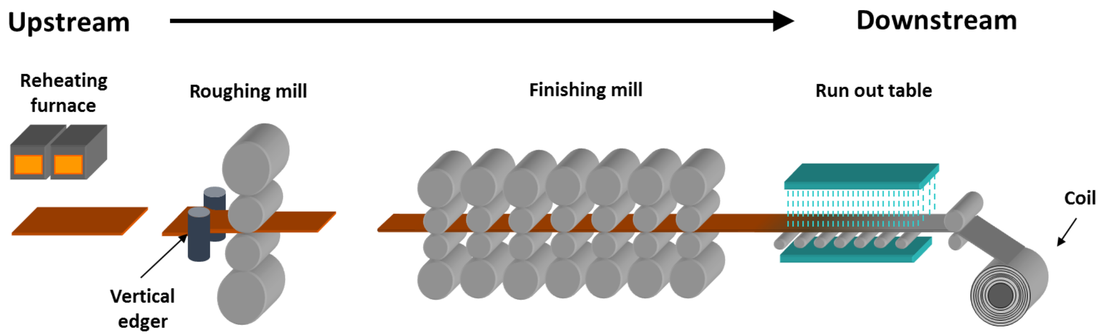

Figure 1: Overview of conventional hot rolling mill [6]

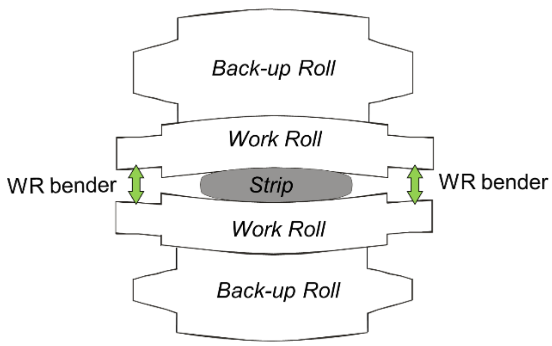

Figure 2: 4-high rolling mill diagram

3 STRIP CROWN CALCULATION

3.1 Strip profile and strip crown

During the rolling process, when a large rolling load is applied to the stand, the WR and

BUR are elastically deformed. Due to this deformation, the distribution of strip thickness along the width (hereinafter strip profile) changes. The strip crown is the difference in thickness between the center and the point near the edge of the strip as Figure 3. In this study the measured point from the edge is 40 mm (C40). The strip crown can be calculated from the following equation:

$$C = h_C - \frac{h_W + h_D}{2} \tag{1}$$

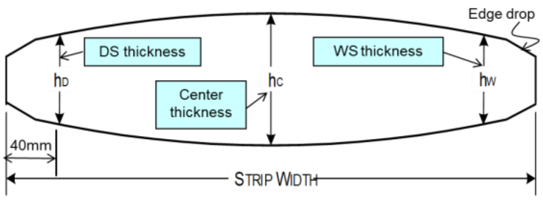

Figure 3: Strip profile

3.2 Online strip crown model

To control the strip crown during the online hot rolling process, it is necessary to calculate strip crown model in a short time cycle. Therefore, a simplified model formula (online strip crown model) is used. In this model, several factors should be considered to improve strip crown control accuracy. The strip crown ratio $\frac{C_i}{h_i}$ on the exit side of each stand is a dimensionless quantity obtained by dividing the strip crown $C_i$by the strip thickness h_i and is calculated by the following equation:

$$\left(\frac{C_i}{h_i}\right) = \eta_i \cdot \left(\frac{C_{i-1}}{h_{i-1}}\right) + \xi_i \cdot \left(\frac{C_i^{UFD}}{h_i}\right) \tag{2}$$

where, η_i is heredity coefficient, ξ_i is transcription coefficient and i is the stand number. Here, $C_i^{UFD}$is the strip crown calculated from the case with uniform force distribution (UFD) in strip width direction. Figure 4 shows a diagram for a UFD model. In a UFD model, because the rolling force is uniform, the reduction is assumed to be uniform. So, assuming constant tensile stress, the strip crown ratios of entry and exit sides are assumed to be equal. The strip crown with UFD model can be expressed as:

$$C^{UFD} = func(F^R, F^B, B, E^{WR}, D^{WR}, D^{BUR}, C^{WR}, C^{BUR}) \tag{3}$$

where,

C^{UFD}	: UFD strip crown	C^{WR}	: WR initial crown
B	: Strip width	C^{BUR}	: BUR initial crown
F^R	: Rolling force	D^{WR}	: WR diameter
F^B	: Bending force	D^{BUR}	: BUR diameter
E^{WR}	: WR elastic modulus		

In UFD crown, a value close to the theoretical value can be obtained by determining the coefficient of the UFD crown model using a split model, that divides the roll axis direction into

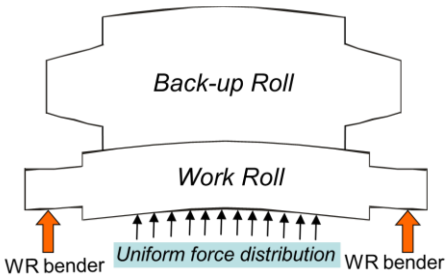

Figure 4: UFD model diagram

a large number of elements and calculates the balance between the elements by iterative calculation [2, 3]. The crown ratio heredity coefficient is a parameter that expresses the effect of the entry side crown ratio on the exit side crown ratio. The transcription coefficient is a parameter that indicates the effect of the UFD crown on the exit side crown ratio.

Conventionally, crown ratio heredity coefficient and transcription coefficient analysis has been carried out based on experimental results using an experimental rolling mill, but it is not easy to reproduce the rolling conditions in an actual HSM. In addition, since only one profile gage is installed on the exit side of the final stand for six or seven rolling stands, identifying the heredity coefficient and transcription coefficient by a statistical method using actual rolling data is impracticable. Moreover, Ogawa et al. [7] proposed an empirical model that calculated the crown ratio heredity coefficient. In this model, the heredity coefficient can be calculated according to roll and strip geometries and has a good agreement to experimental results in typical rolling conditions.

3.3 Analysis of Crown ratio heredity coefficient and transcription coefficient by FEM

From FEM simulation results of each stand, the crown ratio heredity coefficient and transcription coefficient can be identified by using Equation (2). First, under the same rolling conditions, only the entry side strip crown is changed, and two simulations are performed (hereinafter referred to as Case A and Case B). Since the rolling conditions are the same, by substituting each simulation result into Equation (2), the following two equations are obtained.

$$\begin{aligned} \left(\frac{C_{A,i}}{h_i}\right) &= \eta_i \cdot \left(\frac{C_{A,i-1}}{h_{i-1}}\right) + \xi_i \cdot \left(\frac{C_i^{UFD}}{h_i}\right) \\ \left(\frac{C_{B,i}}{h_i}\right) &= \eta_i \cdot \left(\frac{C_{B,i-1}}{h_{i-1}}\right) + \xi_i \cdot \left(\frac{C_i^{UFD}}{h_i}\right) \end{aligned} \tag{4}$$

By subtracting both sides of above equations, the heredity coefficient η_i can be calculated as:

$$\eta_i = \frac{h_{i-1}}{h_i} \cdot \frac{C_{B,i} - C_{A,i}}{C_{B,i-1} - C_{A,i-1}} \tag{5}$$

Similar to above conditions, by using different WR initial crown (Case C), and substituting the simulation results into Equation (2), the transcription coefficient ξ_i can be calculated as:

$$\xi_i = \frac{C_{C,i} - C_{A,i}}{C_{C,i}^{UFD} - C_{A,i}^{UFD}} \tag{6}$$

where $C_{C,i}^{UFD}$ and $C_{A,i}^{UFD}$ are the UFD profiles with two different work roll crowns. Since the rolling conditions (strip width, force, etc.) are the same and a uniform force distribution is assumed, the rolls deflection and flattening will not change, and only the roll initial crown will be changed. Therefore, Equation (6) can be written as:

$$\xi_i = \frac{C_{C,i} - C_{A,i}}{C_{C,i}^{WR} - C_{A,i}^{WR}} \tag{7}$$

where $C_{C,i}^{WR}$ and $C_{A,i}^{WR}$ are the work roll ground crowns.

4 ANALYSIS METHOD

4.1 FEM model

In this study, the deformation of strip and rolls during the rolling process was analyzed using the finite element method based on the dynamic explicit solver (LS-DYNA*) which is suitable for the analysis of large deformation. Figure 5 shows the model of a 4-High rolling mill. To shorten computing time, here we have considered 1/4 model. The strip is symmetrical in the thickness and width directions, WR and BUR is symmetrical in the roll length direction. The WR and BUR dimension are plotted in Table 1. In this simulation we have calculated the strip crown for stand F3, F4 and F5 with flat strip, strip with entry crown and WR initial crown. In all stands, the same model with different strip thickness was used.

The penalty method was applied to the contact area between WR-strip and WR-BUR. In the penalty method, artificial interference springs are placed normal to the contacting surfaces on all the penetrating nodes.

Table 1: WR and BUR dimensions for 1/4 FEM model (Full model dimensions in parentheses)

Roll	Barrel diameter Db [mm]	Neck diameter Dn [mm]	Barrel length Lb [mm]	Neck length Ln [mm/side]
WR	800	600	940 (1880)	480
BUR	1500	1050	780 (1560)	590

4.2 Physical properties

The material type of elasto-plastic material was applied to the strip material. The elasto-plastic body is a material type that has the property that it elastically deforms below the yield stress and plastically deforms above the yield stress. For WR and BUR, the material type of elastic body was applied. Since the elastic body does not consider the yield phenomenon, it has a feature that the calculation time is short. Tables 2 and 3 show the mechanical properties of the rolls and strip (low carbon steel) used in these simulations.

Table 2: Material properties of strip

Young's modulus *E* [GPa]	Poisson's ratio ν	Density *ρ* [ton/mm^3]	Material constant *K* [MPa]	Strain hardening coefficient *m*
120	0.3	7.85×10^{-9}	240	0.21

* Trademark of Livermore Software Technology Corporation

Table 3: Material properties of WR and BUR

Young's modulus *E* [GPa]	Poisson's ratio ν	Density ρ [ton/mm^3]
210	0.3	7.85x10^{-9}

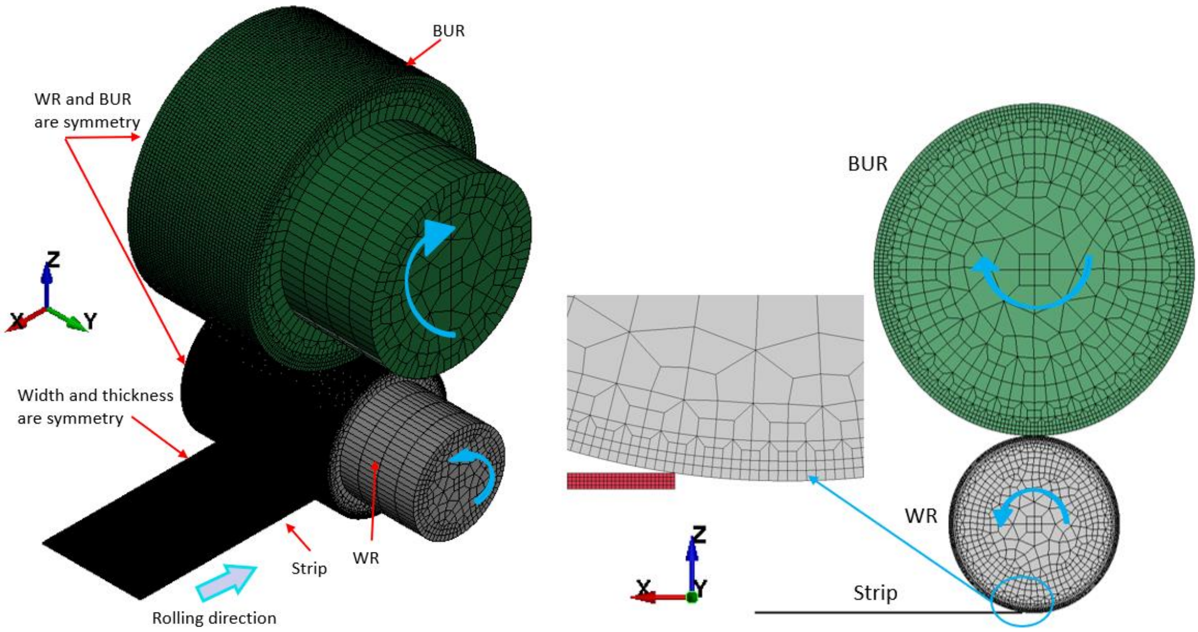

(a) Isometric view (b) Side view

Figure 5: 4-High rolling mill (1/4 FEM model)

4.3 Analysis conditions

In this study, a total of 9 cases were simulated. The analysis conditions are shown in Table 4. In every stand, three cases A, B and C have been used to calculate the crown ratio heredity coefficient and transcription coefficient. In all cases, the strip width is 1280 mm. By using the symmetry condition, the strip width of the model was set to half the strip width (640 mm). First, we have calculated a model which the strip has no entry crown (flat) and no WR initial crown (straight roll). Then, the entry crown (2% of the entry thickness) was used in entry side of strip. In addition to that, a negative roll crown (-400 µm per diameter) was used in WR. In all cases, the strip length was 1250 mm. The rotational speed of the WR was assumed to be constant (15 rad/s = 6 m/s). The same value of deformation resistance (Table 2) is used for each stand. The friction coefficient between the strip -WR and WR-BUR is 0.3.

Furthermore, to know the bending force effect on the strip crown, we have applied 650 kN/neck bending force in the neck of the WR. Here we have only evaluated the bending force effect on the strips with entry crown (2% entry thickness) for stand F3, F4 and F5.

In a tandem rolling process, since the loopers are existed between the finishing mill and these loopers are controlling the rolling speed and interstand tension. The interstand tension (backward/forward) may have effect on the strip crown. In this part, we have applied uniform backward tension in the tail of strip with entry crown (same as bending force, 2% entry thickness) under rolling conditions of stand F3, F4 and F5.

Table 4: Strip dimensions before and after rolling of strip material (Full model dimensions in parentheses)

Case	Stand	Entry thickness *H* [mm]	Exit thickness *h* [mm]	WR crown [μm/Dia.]	Strip entry crown [μm]	Reduction *r* [%]
1A	F3	8.0 (16.0)	5.0 (10.0)	0.0	0.0	37%
1B				0.0	+160 (+320)	
1C				-400	+160 (+320)	
2A	F4	3.0 (6.0)	2.5 (4.0)	0.0	0.0	37%
2B				0.0	+80 (+160)	
2C				-400	+80 (+160)	
3A	F5	3.0 (6.0)	2.0 (4.0)	0.0	0.0	33%
3B				0.0	+60 (+120)	
3C				-400	+60 (+120)	

5 SIMULATION RESULTS

5.1 Calculated strip crown

To calculate the full length of a strip, it took a long computing time to evaluate different parameters effects on strip crown. Here, due to time constraints, we have continued the simulation up to near half of strip length. The simulation was stopped when a steady state condition was reached.

Figures 6 (a), (b) and (c) show the calculated strip profile for F3, F4 and F5, respectively. In each stand, when the strip entry crown and WR initial crown were used, the strip profile increased. In these simulations due to symmetry condition, half thickness was considered for simulation, the strip profile in Figure 5 is calculated for half thickness. The calculated strip crown for all cases are plotted in Table 5.

Figure 7 shows the bending force and backward tension effects on the strip crown. Here in these figures, we have only calculated the cases having strip entry crown (2% of strip entry thickness) and straight rolls. The strip crown reduced when the bending force was applied. However, comparing the simulation results with and without backward tension, the strip crown reduction is very small. For the viewing convenience, the FEM calculation results of surface nodes displacement are linearly interpolated and shown in Figures 6 and 7. The calculated strip crown for the cases with and without bending force and back tension are plotted in Table 6.

Table 5: Calculated strip exit crown (Full model dimensions in parentheses)

Case	Stand	Entry thickness *H* [mm]	Exit thickness *h* [mm]	WR crown [μm/Dia.]	Strip entry crown [μm]	Strip exit crown C40 [μm]
1A	F3	8.0 (16.0)	5.0 (10.0)	0.0	0.0	106 (212)
1B				0.0	+160 (320)	131 (262)
1C				-400	+160 (320)	199 (398)
2A	F4	3.0 (6.0)	2.5 (4.0)	0.0	0.0	69 (138)
2B				0.0	+80 (160)	92 (184)
2C				-400	+80 (160)	128 (256)
3A	F5	3.0 (6.0)	2.0 (4.0)	0.0	0.0	40 (80)
3B				0.0	+60 (120)	62 (124)
3C				-400	+60 (120)	104 (208)

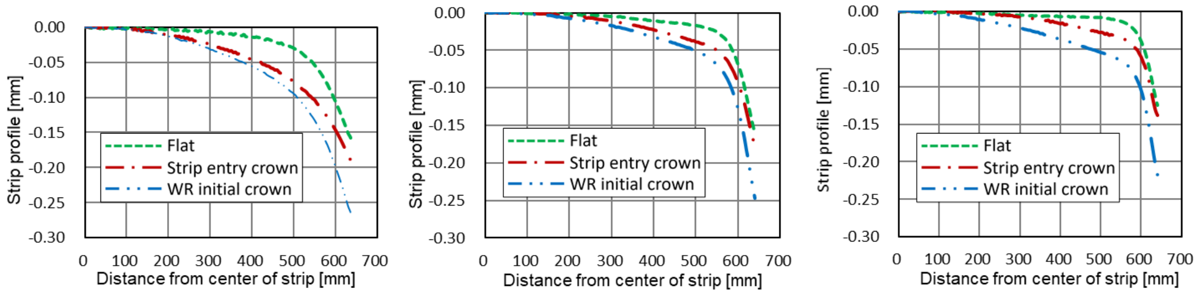

(a) Stand F3 **(b)** Stand F4 **(c)** Stand F5

Figure 7: Strip profile distribution in width direction

Table 6: Calculated strip exit crown with/without bending force and backward tension (Full model dimensions in parentheses)

Case	Stand	Entry thickness *H* [mm]	Exit thickness *h* [mm]	Bending force [kN/neck]	Backward tension [MPa]	Strip exit crown C40 [μm]
1A	F3	8.0 (16.0)	5.0 (10.0)	0.0	0.0	131 (262)
1B				650.0	0.0	108 (216)
1C				0.0	10.0	126 (200)
2A	F4	4.0 (8.0)	2.5 (5.0)	0.0	0.0	92 (184)
2B				650.0	0.0	79 (158)
2C				0.0	12.0	91 (182)
3A	F5	3.0 (6.0)	2.0 (4.0)	0.0	0.0	62 (122)
3B				650.0	0.0	48 (96)
3C				0.0	14.0	61 (124)

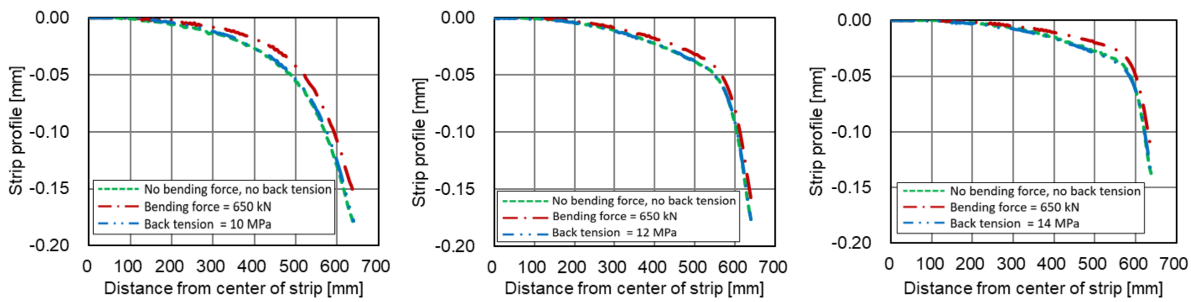

(a) Stand F3 **(b)** Stand F4 **(c)** Stand F5

Figure 7: Effect of bending force and backward tension on strip profile

5.2 Roll axial deflection and roll flattening deformation

In this study, all components of the rolling mill are subjected to elastic deformation caused by the rolling force. In a 4-High rolling mill, four kinds of deformations, WR axial deflection, BUR axial deflection, WR-strip flattening deformation and WR-BUR flattening deformation are present. Here, in this part the amounts of all these deformations have been analyzed numerically.

Figures 8 and 9 show the WR and BUR center axial deflections of F3, F4 and F5, respectively. The horizontal axes represent the axial position from the roll center to the roll neck, and the vertical axes represent the roll deflection. In each stand, the WR deflection increased by using strip entry crown and WR initial crown. However, the BUR axial deflections are nearly same in each stand with with/without strip entry crown and WR initial crown.

Figure 10 represents the contact flattening deformation between WR-strip for stands F3, F4 and F5, respectively. Here, similar to WR deflection, the contact flattening deformation increased by using strip entry crown and WR initial crown. The cases with only strip entry crown have smaller flattening deformation in the strip edge side and larger in the strip center. The flattening deformation is high in the case with WR initial crown. Since the WR-strip flattening deformation has a direct effect on the strip crown, as has been previously shown the strip crown is large in the cases with WR initial crown.

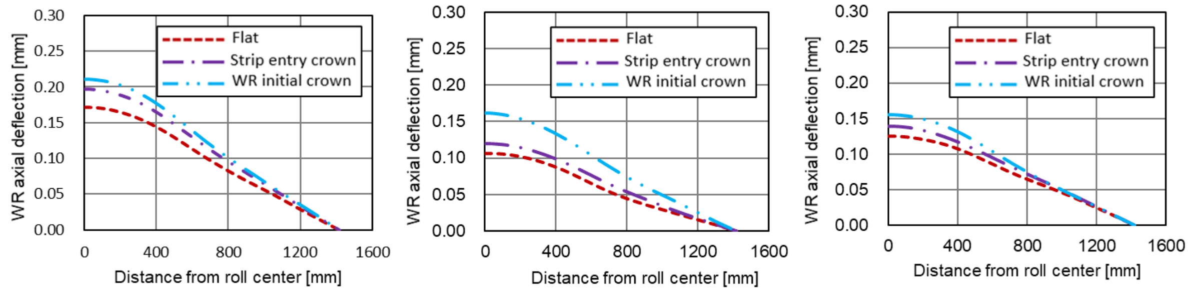

(a) Stand F3 **(b)** Stand F4 **(c)** Stand F5

Figure 8: Effect of strip entry crown and WR initial crown on WR axial deflection

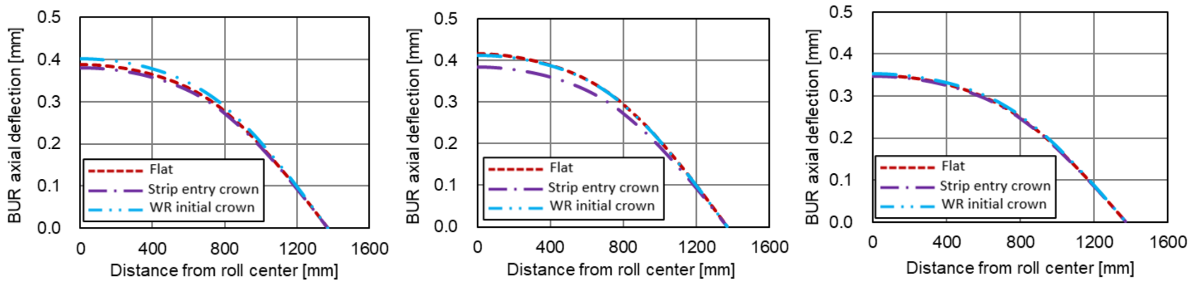

(a) Stand F3 **(b)** Stand F4 **(c)** Stand F5

Figure 9: Effect of strip entry crown and WR initial crown on BUR axial deflection

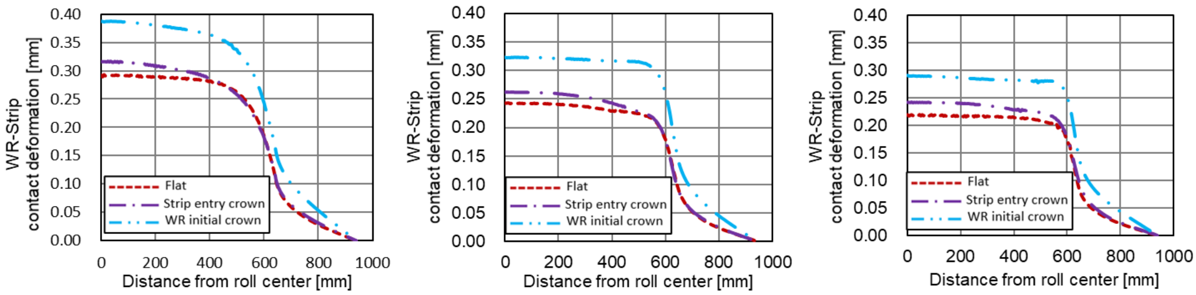

(a) Stand F3 **(b)** Stand F4 **(c)** Stand F5

Figure 10: Effect of strip entry crown and WR initial crown on WR-strip contact flattening deformation

As explained in previous section, the effect of bending force and backward tension were evaluated on the flat strip and straight rolls for stand F3. Figure 11 show the roll deflections and roll flattening deformations. Here similar to the strip profile, WR deflection has not changed when backward tension was applied. However, the WR axial deflection changed when the bending force was applied on the neck of WR. Furthermore, WR flattening deformation also significantly changed in the case with bending force.

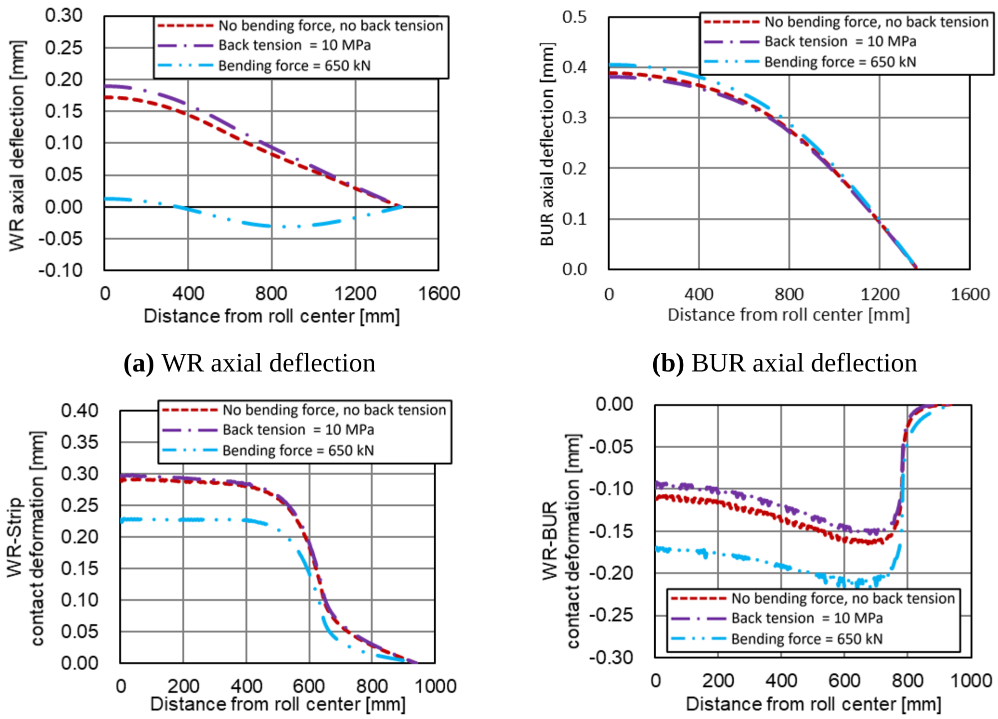

(a) WR axial deflection **(b)** BUR axial deflection

(c) WR-strip contact deformation **(d)** WR-BUR contact deformation

Figure 11: Effect of bending force and backward tension on the roll axial deflection and roll flattening

5.3 Equivalent stress distribution during WR and strip contact

To know the contact stress distribution on the surface of strip, the calculation results of equivalent stress (von Mises stress) distributions during contact between the strip and WR were compared. Equivalent stress shows yield stress when plastic deformation occurs and widely used to know the plastic deformation region. In F3, F4 and F5, only the results of the case without entry crown (flat strip and straight roll) are plotted. Figure 12 show the equivalent stress distribution during contact at time of t = 0.05s (when the simulation became stable). Here, in these figures the horizontal axes of x show the longitudinal position. As the origin (x = 0) is at the position directly below the roll axis (center), the direction from the WR center to the exit side is positive (x > 0) and the direction from the WR center to the entry side is negative (x < 0). The plotted points in width direction are 40 mm form the edge, 300 mm from the edge and center of strip.

From entry side to exit side, the equivalent stress increased due to increases of work hardening and shear strain. However, the equivalent stress value decreases near the neutral point.

It is thought that this is due to the strip and roll surfaces not slipping relative to each other, with no frictional force generation. Also, the vicinity of the neutral point surrounded by the shear deformation area cannot be deformed because the required shear stress for deformation is saturated. The equivalent stress distributions are almost uniform in the strip width direction, however small deviations exist in stand F5. This seems to be mainly due to the width spread of the strip.

Moreover, the same number of slices are used in strip thickness direction for all stands, and when the reduction is small, a finer mesh should be used. In these simulations, it looks as if the mesh size is too coarse in F5.

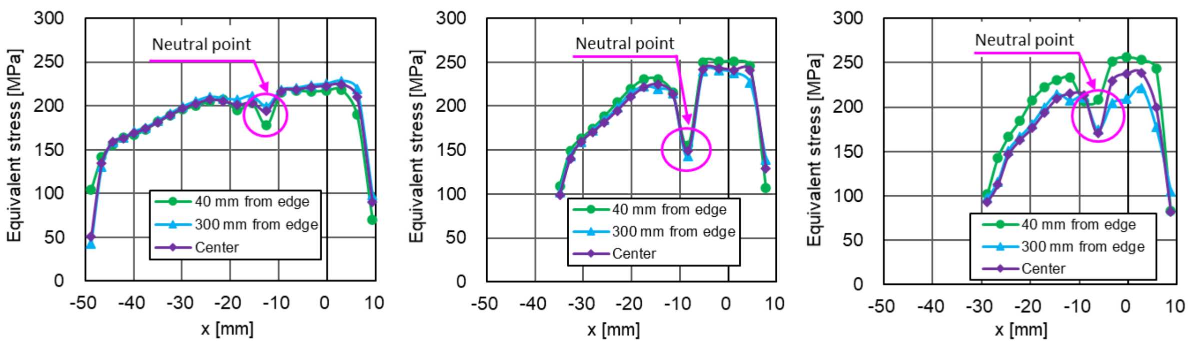

(a) Stand F3 **(b)** Stand F4 **(c)** Stand F5

Figure 12: Equivalent stress distribution in longitudinal direction

5.4 Calculated crown ratio heredity coefficient and transcription coefficient

The strip crown ratio heredity coefficient and transcription coefficient were calculated from the FEM simulation results of each stand by using Equations (5) and (7). Figure 13 shows the relationship between the calculated crown ratio heredity coefficient and the strip width/strip entry thickness ratio (B/H). In the figure, the crown ratio heredity coefficient was calculated from the strip crown selected from two different points 40 mm (C40) and 75 mm (C75) (from the edge of the strip). The calculated values were compared to the data calculated by the Ogawa model (green solid line) and a good agreement has been seen, as shown in Figure 13.

Figure 14 shows the relationship between the calculated heredity coefficient and transcription coefficient. According to the Ogawa model [7], the sum of the heredity coefficient and the transcription coefficient is 1 ($\eta + \xi = 1$) when entry and exit crown ratios are same. Comparing these two coefficients, the plotted data should overlap each other. However, a little deviation can be seen, and this may be due to slight differences in crown ratios in entry and exit sides and the influence of mesh size specially around the contact surface.

Further work is required to investigate the effects of other parameter variations, such as the influence of width spread due to change of strip crown ratio, friction coefficient and so on.

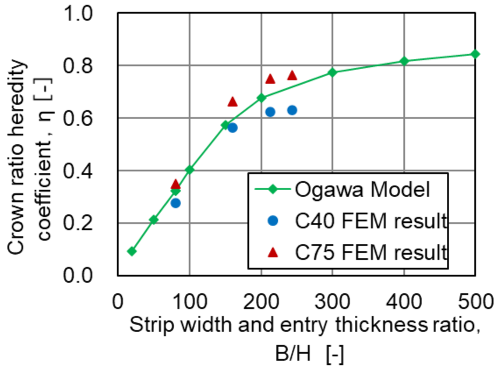

Figure 13: Relationship between crown ratio heredity coefficient and strip width ratio

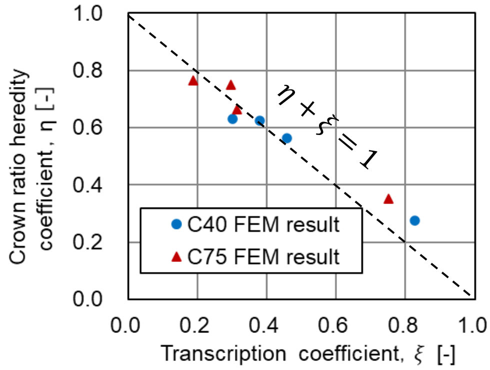

Figure 14: Relationship between calculated crown ratio heredity coefficient and transcription coefficient

6 CONCLUSIONS

A FEM model based on the dynamic explicit method was developed that can analyze the elastic deformation of the roll and elastic plastic deformation of strip under different rolling conditions for a general 7-stand finishing mill. The simulations were performed by using flat strip, strip with entry crown and WR initial crown for stands F3, F4 and F5. The crown ratio heredity coefficient and transcription coefficient were calculated by using the simulation results. The analysis results had a good agreement compared to the empirical model by Ogawa et al. [7]. Additionally, the effects of bending force and back tension were evaluated on the strip crown. By applying bending force, the strip crown was decreased. However, there was not significant change in the strip crown by applying back tension.

REFERENCES

[1] M. D. Stone, and R. Gary, Theory and Practice Aspects in Crown Control. AISE Yearly Proceeding (1965) 657-674.

[2] K. N. Shohet and N. A. Townsend, Roll bending methods of crown control in four high plate mill, J. Iron & Steel Inst. (1969) 37:1088-1098.

[3] J. Yanagimoto, T. Sasaki, M. Kiuchi and T. Kono, Three-Dimensional Coupled Simulation Technique for Strip Rolling Processes and Experimental Verification of Accuracy of Numerical Results: Research on Computational Rolling Mill III, J. Jap. Soci. Tech. Plast. (1992) 33 (383):1406-1411(in Japanese).

[4] Y. Mitai, Y. Hongo and Y. Oshima, Analytical Study on the Hereditary Characteristic of Crown-Ratio by Hot-Rolling of Strip Using Three-Dimensional Rigid Plastic FEM, J. Jap. Soci. Tech. Plast. (2000) 41 (470): 217-221(in Japanese).

[5] H. Yoneda, M. Kitahama and M. Shitomi, Development of Profile and Flatness Control Models and Application to Mizushima Hot Strip Mill, KAWASAKI STEEL, Technical report (1996) 28(2):82-88 (in Japanese).

[6] M. Sekimoto, M. Sano and K. Ohara, Modelling of Width Control for Hot Strip Mill with FEM Analysis, COMPLAS Proceeding (2019) 59-67.

[7] S. Ogawa, H. Matsumoto, S. Hamauzu and T. Kikuma, On-line calculation method of strip crown in hot strip mills. J. Jap. Soci. Tech. Plast. (1984) 25(286):1034-1041 (in Japanese).